International Journal Multidisciplinary
Homepage : https://journal.antispublisher.com/index.php/IJMI
Email : admin@antispublisher.com

e-ISSN : 3031-9870
IJMI, Vol. 3, No. 3, August 2026
Page 96-104

Preparation of Superparamagnetic Calcium Ferrite Nanoparticles using Solid State Technique and Analysis of Their Structural Properties

Robak Aziz Rashid[1], Dheyab T. Noori[2], Raham Z. Hadi[3]
[1,2,3]College of Education, Tikrit University, Iraq

DOI : https://doi.org/10.61796/ijmi.v3i3.545

Sections Info

Article history:
Submitted: May 05, 2026
Final Revised: June 20, 2026
Accepted: July 15, 2026
Published: August 03, 2026

Keywords:
Spinel ferrite
X-Ray
VSM
FT-IR
FE-SEM
Nanoparticle size
Magnetic field

ABSTRACT

Objective: *In the current experiment, the preparation and characterisation of calcium ferrite nanoparticles has been performed using solid state technique by the use of iron nitrate and calcium nitrate in equimolar quantities, which have been mixed using ethylene glycol. Influence of temperature, preparation technique, duration of calcination of granules and presence of air in laboratory atmosphere has also been studied.* ***Method:*** *In the current experiment, the preparation and characterisation of calcium ferrite nanoparticles has been performed using solid state technique by the use of iron nitrate and calcium nitrate in equimolar quantities, which have been mixed using ethylene glycol.* ***Results:*** *Initially, X-ray diffraction results showed that the optimum temperature for phase growth and the onset of single-phase calcium ferrite nanoparticles was 400 °C with an exposure time of 4 hours; infrared spectroscopy results revealed the presence of functional groups, and the type of bonds in the structure was identified. As for the scanning electron microscopy results, these revealed the presence of distinctive spherical shapes in the nanoparticles. The results of this analysis also showed that as the sintering temperature increased, the nanoparticle size increased without affecting the spherical shape. The magnetic properties of the samples were also examined; the results revealed magnetic relaxation loops for the nanoparticles at different temperatures. It was found that the coercive magnetic field was zero, and it was also found that the nanoparticles exhibited superparamagnetic properties.* ***Novelty:*** *Influence of temperature, preparation technique, duration of calcination of granules and presence of air in laboratory atmosphere has also been studied.*

INTRODUCTION

Currently, magnetic nanoparticles have received considerable interest from the scientific community due to their various uses, including delivery of drugs to a targeted location in the body, diagnosis of various ailments, water treatment, chemical catalysts, computers' memory and sensors [1,2]. Of these applications, spinel ferrite nanoparticles have received a lot of attention due to their exceptional magnetic and electrical characteristics [3]. Moreover, because of their minute sizes, these nanoparticles could possess some special physical and chemical characteristics compared to larger materials [4]. The first investigation into the influence of size on the magnetic characteristics of ferrite nanoparticles was done by Tang et al. in 1991 [5]. Particle shape, size, and particle size distribution play very important roles in defining their physical and chemical properties [6]. Most spinel ferrites display superparamagnetic properties at nanometer sizes below or around 20 nanometers [7]. Research into the properties is heavily dependent on the size of the ferrite espinel nanoparticles and the magnetic field used. It is therefore important to understand this concept in order to know how large and small nanoparticles are affected magnetically. The most complicated property of particle size is that which affects magnetic properties of the substance. Magnetic particles and non-

magnetic substances of small sizes have unique properties affected by quantum behavior that is associated with the particle size. When the particle size is smaller than the domain size of the material, this results in changes in the magnetic properties of the substance. Here, because of the small particle size and sharp drop in the number of parallel spins that face the same direction, the resultant magnetic moment in these nanoparticles is small enough to overcome temperature fluctuation; in other words, the magnetic force is weakened by the temperature fluctuation. Because of this, when plotting M against H of superparamagnetic substances, there is no observable magnetic slowing down. When a magnetic field is applied to a substance that has superparamagnetic properties, the magnetic moments align perfectly and very quickly with the field until the point of magnetic saturation is reached; without the field, they rapidly lose their magnetic properties [8-14] The ferrites are usually synthesized by a ceramic route or solid-state reaction above the temperature of reaction of oxides and carbonates. In this route, the particle size is large and non-uniform along with the presence of other phases and impurities that affect the performance of products [15–17]. In order to overcome the above-mentioned limitations and meet the requirements of new applications, some wet chemical techniques such as sol–gel technique [18], hydrothermal synthesis [19], reverse microemulsion route [20], and co-precipitation [21] have been used for the synthesis of ferrite nanoparticles having appropriate magnetic properties. All these methods have one that has grabbed the interest of the scientific community due to its high availability, lower costs, control of the end product, and purity [23-22]. Controlling the size, shape, and surface area of the particles is usually a very difficult process. The environmental factors such as atmosphere, synthesis conditions, temperature, sintering time, speed of mixing, concentration of reactants, pH, and types of salts used (chlorides, nitrates, and sulphates) can be very important factors in controlling particle sizes and structural parameters associated with crystallization [24]. Regarding this topic, Jani et al. [25] investigated the preparation of calcium ferrite nanoparticles via self-ignition "sol-gel" and mixing solutions method. The synthesis method has been proven to affect the surface morphology, shape, and structure of the synthesized nanoparticles. For instance, in the study done by Suleiman et al. [26], the researchers synthesized calcium ferrite nanoparticles from the precursors of calcium and iron with citric acid nitrate using the sol-gel method. From XRD analysis, it was established that there is the formation of a tetragonal structure of the calcium ferrite nanoparticles while the result from the VSM shows the superparamagnetic behavior of the nanoparticles with saturation magnetization of 88.3 emu/g. Suleiman et al[27].

RESEARCH METHOD

Materials and preparation methods for particle synthesis

Calcium spinel ferrite nanoparticles were synthesized using ferric nitrate trihydrate ($Fe(NO_3)_3 \cdot 9H_2O$) and calcium tetranitrate ($Ca(NO_3)_2 \cdot 4H_2O$) as raw materials; deionised water and ethylene glycol were used as solvents. All materials utilized in this study were bought from Samchum in the form of high purity. The materials were weighed to an

accuracy of 0.0001 g and sample preparation was done using electric furnace, Azar Kore Model PX-9 machine and X'Pert Pro (XRD) produced by Panalytical, a Dutch Company. The machine was run using Cu anode with a wavelength (λ = 1.54056 Å) at 40kV and 30mA, with a scan rate of 0.05°/s from 10° < 20 ≤ 80° to identify the phase of the samples. For microstructure and morphology analysis of the samples, a field emission scanning electron microscope produced by the Czech Company TESCAN and a Hitachi HT7800 transmission electron microscope produced by the Japanese Company Hitachi were used. An AVATAR Fourier transform infrared (FT-IR) spectrometer was used to analyze molecular bands and functional groups. Calcium ferrite was synthesized by the ceramic process. Oxides of high purity levels of 99.99% CaO and Fe were used as starting materials. The metal oxide ions were blended depending on their molecular ratios. The sample was subsequently powdered; the powder blend was put in an electric ball mill for 48 hours and thereafter subjected to pressing and sintering at 800°C for two hours in °C/min heating rate. This was done to enable the first stage of chemical reaction among the constituent elements.

RESULTS AND DISCUSSION

A. X-ray Abnormality Test Results

Figure 1 shows the X-ray diffraction pattern of samples prepared at different temperatures, with a sintering time of four hours; this time was taken as the onset of phase formation. The results indicate that all samples exhibit a single phase at different temperatures, with the diffraction peaks identified and recorded in Table (1). The diffraction peaks at (311), (220), (031), (400), (331), (422), (511) and (440). These planes confirm the formation of a spinel structure, and no impurities or other anomalous phases were observed; these phases correspond to the International Standard Card (01-085-1436) This information enables us to utilise different diffraction patterns in various methods and stages, and reveals the average crystal sizes and the determination of lattice parameters. The absence of impurities in the sample is attributable to the success of the preparation process and the conditions under which the samples were produced. The diffraction patterns were identified and matched using the X-pert software, and the predominant phase was found to be calcium feldspar. the average crystallite sizes for each sample were determined using Scherers [28]:

$$D = \frac{k\lambda}{\beta \cos\theta} \quad \ldots\ldots\ldots\ldots\ldots\ldots\ldots\ldots\ldots\ldots\ldots\ldots (1)$$

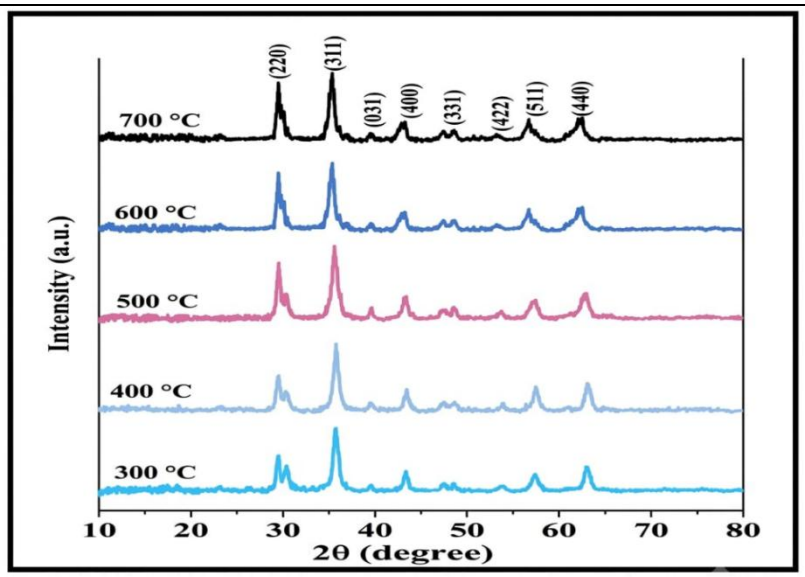

Figure 1. X-ray diffraction patterns of samples prepared at different temperatures over a period of 4 hours using the solid-state method.

Table 1. Lattices constants and crystal size distributions for samples prepared at various temperatures for 4 hours using the solid-state method

Calcination temperatures (°C)	Constants of the crystal lattice (A°)	Crystalline size ratio (nm)
300	8.22	7
400	8.20	11
500	8.17	14
600	8.13	16
700	8.9	19

B. Results of infrared spectroscopic analysis

Infrared spectra of the dry nanocomposite of the calcium feldspar particles at different temperatures for the samples that were sintered at different temperatures as shown in the examination image are shown in Figure 2. Calcination time is 4 hours; absorption peak at wavenumber 1394 cm^{-1} is the bending vibration of the nitrate group, while the peak at 1624 cm^{-1} is the carboxyl group vibration. In the range between 300 and 700 Celsius temperature, two important peaks appear at 400-600 cm^{-1}, both corresponding to the oxygen bond. Two peaks are representing the spinel structure of the ferrite prepared; namely, the higher peaks at wavenumbers 593, 594 and 596 cm^{-1} are the stretching vibrations of the metal-oxygen bond in the tetrahedral structure, while the lower peaks at wavenumbers 423, 424 and 428 cm -1 are the octahedral vibrations of the metal-oxygen bond.

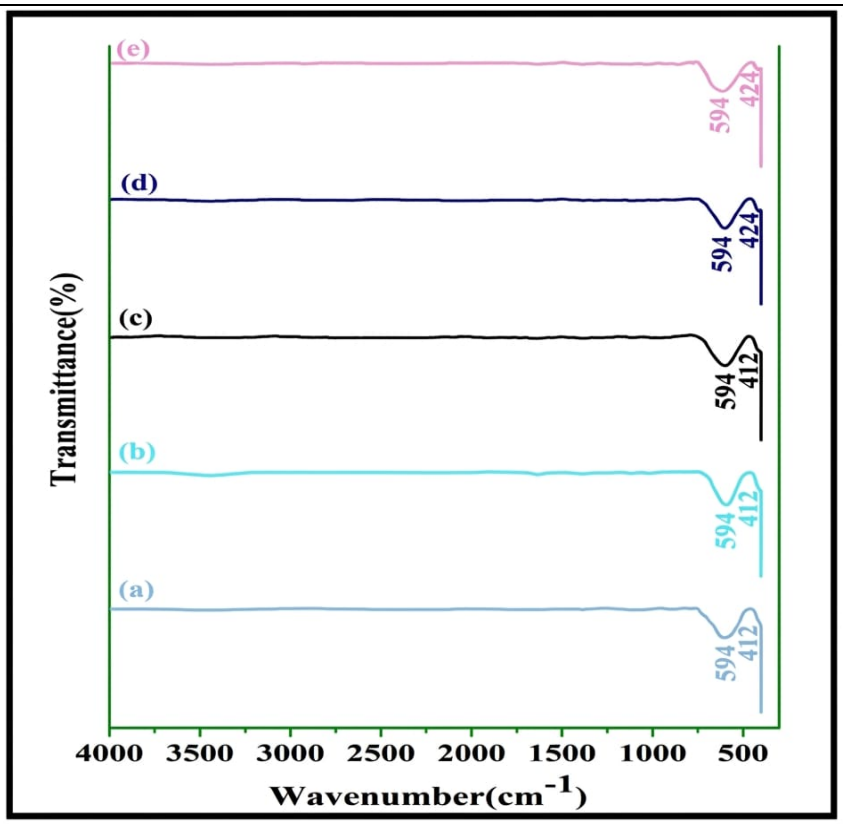

Figure 2. FT-IR Result of Sample in different temperature in 4 hours in solid state method.

C. Results of the scanning electron microscope analysis

Figure 3 shows the samples sintered at different temperatures over a period of 4 hours; each sample is accompanied by a particle size distribution graph based on their nanoscale dimensions. The images reveal that the samples have a distinct spherical shape, with only a very slight change in shape observed as the temperature increases. Their nanoscale sizes at temperatures of 300, 400, 500, 600 and 700 Celsius were approximately 11, 12, 17, 18 and 20 nanometres respectively. At 400 °C, when determining the nanoscale size of the particles, no fewer than one hundred particles were observed. The average sizes were determined using ImageJ software and plotted in Origin Lab version 2021.

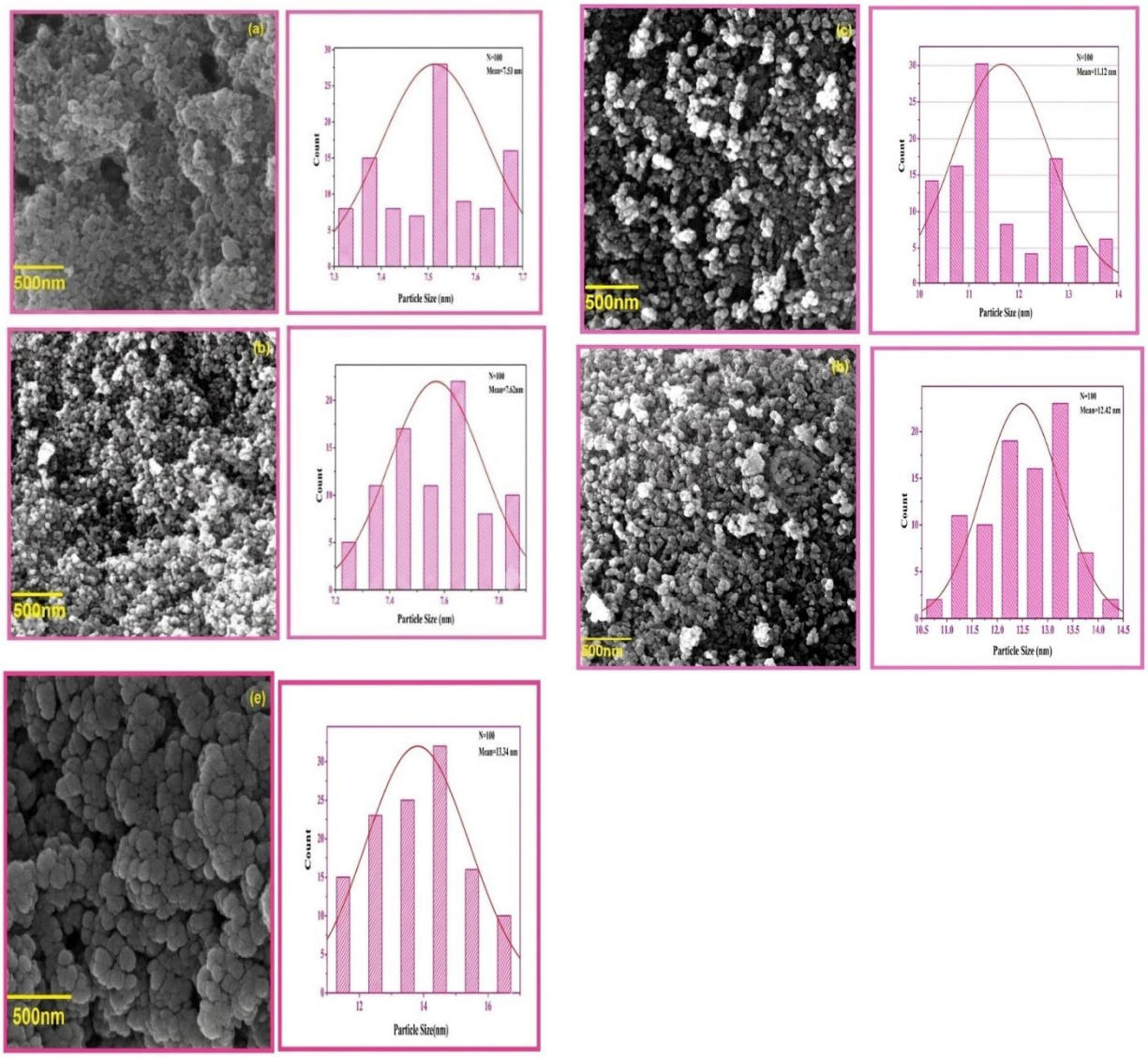

Figure 3. FE-SEM Result of Sample in different temperature in 4 hours in solid state method.

D. Results of the magnetic properties test

Figure 4 shows an increase in the saturation magnetisation value at temperatures of 300 and 400 Celsius, which then decreases gradually as the temperature rises. Cation distribution is considered the most important factor influencing the magnetic properties of the nanoparticles of the prepared calcium ferrite compound, compared to the bulk state of the compound. As the temperature increases, a clear change in the compound's structure is observed, with a transition from inverted spinel to mixed spinel. The figure also shows the magnetic relaxation of the samples prepared and sintered at the temperatures mentioned, where the saturation magnetisation, magnetic coercive force and magnetic relaxation were obtained using Equation (2), from which the coercivity constant (K) was also calculated; the results are presented in Table (2) in accordance with Figure (4) It can be observed that, as the temperature increased, the samples exhibited superparamagnetic properties, as no loop was observed in the magnetic hysteresis loop. This is due to the fact that the size of the nanoparticles reached the critical

superparamagnetic size, as well as their small size, which leads to a decrease in the coercive field to the point where it may even become zero. This is a decrease[29]:

$$K = M_s \frac{H_c}{0.96} \quad \ldots\ldots\ldots\ldots\ldots\ldots\ldots\ldots\ldots\ldots\ldots\ldots\ldots\ldots (2)$$

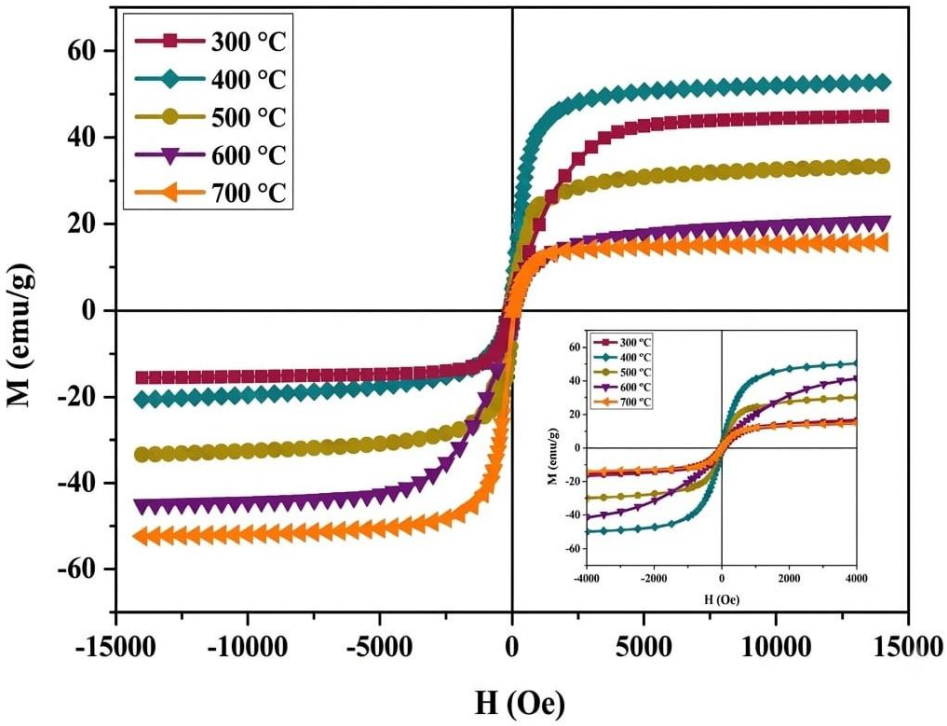

Figure 4. The hysteresis loop for samples prepared at different degrees of calcination over a 4-hour period using the solid-state method.

Table 2. Properties of magnetic for samples prepared at different degrees of calcination over a 4-hour period using the solid-state method.

Calcination temperatures (°C)	K (emu/Oe)	H_c (Oe)	Mr (emu/g)	Ms (emu/g)
300	0	0	1.21	25.23
400	0	0	2.2	44.12
500	0	0	2.3	38.66
600	0	0	0.55	18.32
700	0	0	1.44	10.33

CONCLUSION

Fundamental Finding : In this study, calcium ferrite nanoparticles were characterised and synthesised using the solid-state synthesis method, also known as the ceramic method. Initial X-ray diffraction analysis revealed the presence of layers, as predicted by Bragg's law, based on an analysis of the X-ray reflection results, which formed a monocubic structure. As for the infrared spectrum, the results indicated the presence of functional groups of the oxides of the elements used in the preparation at all temperatures, with the synthesis taking approximately four hours. Furthermore, the

results and scanning electron microscope images showed that the nanoparticles took on spherical shapes of varying sizes; it was observed that as the calcination temperatures increased, so did the nanoscale sizes of the particles. Finally, the results of the magnetic examination of the vibrating samples revealed different behaviours at the temperatures used during the preparation process, which took approximately four hours; the samples exhibited superparamagnetism at all temperatures. **Implication :** The observation that the nanoparticles exhibited superparamagnetism at all temperatures, together with the relationship between calcination temperature and particle size, suggests that the synthesis conditions influence the structural, morphological, and magnetic characteristics of calcium ferrite nanoparticles. **Limitation :** The study examined the nanoparticles prepared under the temperatures used during the preparation process and characterised them using X-ray diffraction, infrared spectroscopy, scanning electron microscopy, and vibrating sample magnetometry. Future **Research :** Future studies may investigate a wider range of synthesis parameters and preparation conditions to further evaluate their effects on the structural, morphological, and magnetic properties of calcium ferrite nanoparticles.

REFERENCES

[1] A. Baykal, I. A. Auwal, S. Güner, H. Sözeri, J. Magn. Magn. Mater., vol. 430, pp. 29, 2017.
[2] A. D. Deshpande, K. G. Rewatkar, V. M. Nanoti, Mater. Today Proc., vol. 4, no. 11, pp. 12174, 2017.
[3] R. B. Jotania, R. B. Khomane, C. C. Chauhan, S. K. Menon, B. D. Kulkarni, J. Magn. Magn. Mater., vol. 320, no. 6, pp. 1095, 2008.
[4] R. A. Nandotaria, R. B. Jotania, C. S. Sandhu, M. Hashim, S. S. Meena, P. Bhatt, S. E. Shirsath, Ceram. Int., vol. 44, no. 4, pp. 4426, 2018.
[5] D. D. Parmar, P. N. Dhruv, S. S. Meena, S. Kavita, C. S. Sandhu, M. Ellouze, R. B. Jotania, J. Electron. Mater., vol. 49, no. 10, pp. 6024, 2020.
[6] V. A. Rane, S. S. Meena, S. P. Gokhale, S. M. Yusuf, G. J. Phatak, S. K. Date, J. Electron. Mater., vol. 42, no. 4, pp. 761, 2013.
[7] P. Kaur, A. Duong, S. K. Chawla, S. B. Narang, S. S. Meena, SN Appl. Sci., vol. 1, no. 10, Art. no. 1239, 2019.
[8] M. A. Almessiere, Y. Slimani, M. Sertkol, M. Nawaz, A. Baykal, I. Ercan, Results Phys., vol. 13, Art. no. 102244, 2019.
[9] Y. Yang, J. Shao, F. Wang, D. Huang, J. Ceram. Process. Res., vol. 18, no. 7, pp. 501, 2017.
[10] F. Nakagomi, P. E. N. de Souza, T. J. Castro, V. K. Garg, A. C. Oliveira, F. C. E. Silva, A. Franco, P. C. Morais, S. W. da Silva, J. Alloys Compd., vol. 842, Art. no. 155751, 2020.
[11] T. J. Castro, P. A. M. Rodrigues, A. C. Oliveira, F. Nakagomi, J. Mantilla, J. A. H. Coaquira, A. Franco Júnior, H. V. S. Pessoni, P. C. Morais, S. W. da Silva, J. Appl. Phys., vol. 121, no. 1, Art. no. 013904, 2017.
[12] S. W. da Silva, F. Nakagomi, M. S. Silva, A. Franco, V. K. Garg, A. C. Oliveira, P. C. Morais, J. Nanopart. Res., vol. 14, no. 4, Art. no. 798, 2012.
[13] P. Shepherd, K. K. Mallick, R. J. Green, J. Magn. Magn. Mater., vol. 311, no. 2, pp. 683, 2007.
[14] M. Aziz, S. Atiq, S. Riaz, S. Naseem, IOP Conf. Ser. Mater. Sci. Eng., vol. 60, Art. no. 012045, 2014.
[15] V. P. Singh, G. Kumar, A. Kumar, R. S. Rai, M. A. Valente, K. M. Batoo, R. K. Kotnala, M. Singh, Ceram. Int., vol. 42, no. 4, pp. 5011, 2016.
[16] F. N. Tenorio Gonzalez, A. M. Bolarín Miró, F. Sánchez De Jesús, C. A. Cortés Escobedo, S. Ammar, J. Magn. Magn. Mater., vol. 407, pp. 188, 2016.

[17] Ch. Mamatha, M. Krishnaiah, C. S. Prakash, Int. J. Adv. Sci. Techn. Res., vol. 5, no. 5, pp. 42, 2015.
[18] N. Suo, A. Sun, L. Yu, Z. Zuo, X. Zhao, W. Zhang, Y. Zhang, L. Shao, Z. Dang, Appl. Phys. A, vol. 126, no. 3, Art. no. 183, 2020.
[19] S. K. Chawla, S. S. Meena, P. Kaur, R. K. Mudsainiyan, S. M. Yusuf, J. Magn. Magn. Mater., vol. 378, pp. 84, 2015.
[20] A. P. Bhat, S. J. Dhoble, D. K. Sahu, K. G. Rewatkar, Mater. Today Proc., vol. 5, no. 10, pp. 22181, 2018.
[21] E. Roohani, H. Arabi, R. Sarhaddi, Int. J. Mod. Phys. B, vol. 32, no. 1, Art. no. 1750271, 2018.
[22] P. Kaur, S. B. Narang, S. Bahel, J. Supercond. Nov. Magn., vol. 32, pp. 3525–3534.
[23] C. S. Ega, B. R. Babu, K. V. Ramesh, M. Sreenivasulu, Y. Purushotham, "Correlation between structural, magnetic and dielectric properties of microwave sintered Ni-Zn-Al nanoferrites," 2019.
[24] H. Li, K. Zhu, K. Lei, T. Xu, H. Wu, "Integrated MEMS toroidal transformer with Ni-Zn ferrite core for power supply on chip," IEEE Trans. Power Electron., vol. 37, no. 9, pp. 10075–10080, 2022.
[25] Y. Gao, Z. Wang, J. Pei, H. Zhang, "Structural, elastic, thermal and soft magnetic properties of Ni-Zn-Li ferrites," J. Alloys Compd., vol. 774, pp. 1233–1242, 2019.
[26] X. Niu, B. Zong, H. Hu, B. Wu, "Influence of Sn4+-substituted on the magnetic properties and power loss of Ni-Zn soft magnetic ferrites," Optik, vol. 134, pp. 135–139, 2017.
[27] E. Macrelli et al., "Modeling, design, and fabrication of high-inductance bond wire microtransformers with toroidal ferrite core," IEEE Trans. Power Electron., vol. 30, no. 10, pp. 5724–5737, 2014.
[28] A. Manikandan, S. A. Antony, R. Sridhar, S. Ramakrishna, M. Bououdina, "A simple combustion synthesis and optical studies of magnetic Zn1−xNixFe2O4 nanostructures for photoelectrochemical applications," J. Nanosci. Nanotechnol., vol. 15, no. 7, pp. 4948–4960, 2015.
[29] H. K. G. Alkhazaali, "Study the electrical and magnetic properties of Ferrite $Ni_{1-x}Zn_xFe_2O_4$ films and their potential use in the magnetic core of transformers," J. Phys. Conf. Ser., vol. 1963, no. 1, Art. no. 012031, 2021.

***Robak Aziz Rashid (Corresponding Author)**
College of Education, Tikrit University, Iraq
Email: Rupak.A.Rasheed@tu.edu.iq

Dheyab T. Noori
College of Education, Tikrit University, Iraq
Email: theyab.thair.tuz@tu.edu.iq

Raham Z. Hadi
College of Education, Tikrit University, Iraq
Email: reham.z.hadi@tu.edu.iq